Density Functional Theory Study on Sum-Frequency Vibrational Spectroscopy of Arabinose Chiral Solutions

Ren-hui Zheng,*,† Wen-mei Wei,‡ and Qiang Shi*,†

State Key Laboratory for Structural Chemistry of Unstable and Stable Species, Institute of Chemistry, Chinese Academy of Sciences, Beijing, People's Republic of China 100080, and Department of Chemistry, College of Basic Medicine, Anhui Medical University, Hefei, Anhui, People's Republic of China 230032

Received: September 16, 2008; Revised Manuscript Received: November 10, 2008

Using time-dependent density functional computations we calculate the doubly resonant IR−UV sum-frequency vibrational spectroscopy and sum-frequency vibrational spectroscopy off electronic resonance for D-arabinose solutions. In comparison with the experimental detection limit, the calculated doubly resonant IR−UV sum-frequency vibrational spectroscopy is strong enough to be detectable.

1. Introduction

Most biological molecules are chiral, and optical activity is often the only practical means to distinguish between enantiomers.[1,2] Recently, optical sum-frequency generation (SFG) in chiral liquids is attracting new interest[3−13] as an effective method for probing molecular chirality. In 1965, Giordmaine first pointed out that the nonlinear optical polarization quadratic in the optical electric fields is shown to occur in optically active liquids and to lead to sum- and difference-frequency generation.[14] In 1966, Rentzepis et al. reported coherent optical SFG in aqueous arabinose ($C_5H_{10}O_5$) solutions where the quadratic sum-frequency polarizability correlated with optical activity was found to be within 1 order of magnitude of the nonlinear polarizability in piezoelectric crystals.[15] In 1993, Shkurinov et al. reported that they had succeeded in repeating Rentzepis' experiment.[16] However, in 2000, Fischer et al. failed to detect SFG from arabinose solutions, and with the results from high-level ab initio computations they concluded that the second-order susceptibility in chiral liquids is much smaller than previously thought.[3] In 2001, Belkin et al. also attempted to measure SFG from a water solution of arabinose, but the results showed that its chiral nonlinearity is below the detection limit even near electronic resonance.[9]

Thus, until now SFG of arabinose chiral solutions has not been observed experimentally. The isotropic part of the sum-frequency hyperpolarizability has been calculated from monofluoro-oxirane and propylene oxide using a sum-over-states approach,[3] in which only electronic transitions are considered, and it is of great interest to predict the sum-frequency vibrational spectroscopy (SFVS) for arabinose chiral solutions theoretically. On the basis of Warshel and co-worker's calculation method of direct Taylor expansion of the electronic transition moment in vibrational normal coordinates,[17,18] Zheng and co-workers[12,13] developed a method to predict SFVS of chiral liquids. In this paper, the doubly resonant IR−UV SFVS and SFVS off electronic resonance on arabinose chiral solutions are investigated using these methods.

The remaining parts of this paper are arranged as follows. In section 2, the computational expressions for SFVS are presented. In section 3, we calculate SFVS for D-arabinose solutions using the time-dependent density functional theory (TDDFT//B3LYP/AUG-cc-pVDZ) with the Gaussian 98 package. When compared to the experimental detection limit, the calculated results indicate that the doubly resonant IR−UV SFVS of arabinose chiral solutions is strong enough and should be detected. Conclusions are drawn in section 4.

2. Theory

In the electric dipole approximation, the SFVS output intensity from a bulk of a chiral medium is expressed into[8−10]

$$I(\upsilon = \upsilon_1 + \upsilon_2) \propto |\chi_B^{(2)}|^2 I_1(\upsilon_1) I_2(\upsilon_2) \quad (1)$$

where $I(\upsilon)$ is the output sum-frequency intensity, $I_1(\upsilon_1)$ is the UV or visible beam intensity at frequency υ_1, $I_2(\upsilon_2)$ is the IR beam intensity at frequency υ_2 scanning over vibrational resonances, and $\chi_B^{(2)}$ is the bulk nonlinear susceptibilities. For an isotropic chiral liquid or solution, in terms of nonlinear hyperpolarizability elements $\alpha_{\sigma\rho\kappa}^{(2)}$ of a molecule, orientational averaging yields[8,10,19]

$$\chi_B^{\text{chiral}}(\upsilon, \upsilon_2) = \frac{N_B L_B}{6\varepsilon_0} \alpha_{\sigma\rho\kappa}^{(2)} \cdot e_{\sigma\rho\kappa} = \frac{N_B L_B}{\varepsilon_0} \langle (\hat{l} \cdot \hat{\sigma}) \alpha_{\sigma\rho\kappa}^{(2)}(\upsilon, \upsilon_2) (\hat{m} \cdot \hat{\rho}) (\hat{n} \cdot \hat{\kappa}) \rangle \quad (2)$$

In the above eq 2, $e_{\sigma\rho\kappa}$ is the Levi−Civita symbol, $\alpha_{\sigma\rho\kappa}^{(2)}$ is the second-order molecular polarizability tensor, (l, m, n) and (σ, ρ, κ) refer to the laboratory and molecular coordinates, respectively, and the dot products between the laboratory and molecule frame are direction cosines, ε_0 is permittivity of free space, and L_B is Lorentz local field correction factor.

In the doubly resonant IR−UV SFVS, υ_2 is resonant with a particular vibrational transition of frequency υ_t and the sum-frequency υ is resonant with an electronic transition. The bulk nonlinear susceptibilities can be expressed into[12]

$$\chi_B^{\text{chiral})}(\upsilon, \upsilon_2) = \frac{N_B L_B}{6\varepsilon_0} \frac{1}{h(\upsilon_t - \upsilon_2 - i\Gamma_{Gg'})} \left[\frac{\partial \mu_z}{\partial Q_t} (\alpha_{xy}^B - \alpha_{yx}^B) + \frac{\partial \mu_y}{\partial Q_t} (\alpha_{zx}^B - \alpha_{xz}^B) + \frac{\partial \mu_x}{\partial Q_t} (\alpha_{yz}^B - \alpha_{zy}^B) \right] \quad (3)$$

where the resonant-enhanced anti-Stokes Raman polarizability $\alpha_{\rho\sigma}^B$ arising from the Raman B term is[12]

* Corresponding authors. Tel.: +86-010-82616163. Fax: +86-010-82616163. E-mail: zrh@iccas.ac.cn (R.-h.Z.), qshi@iccas.ac.cn (Q.S.).
† Chinese Academy of Sciences.
‡ Anhui Medical University.

10.1021/jp808228e CCC: $40.75
Published on Web 12/11/2008

$$\alpha_{\sigma\rho}^{B} = \frac{1}{\sqrt{2}h}\sum_{M}\left[\frac{1}{\upsilon_{MG} - \upsilon - i\Gamma_{Mm}}\times \{b^2\langle G|\mu_\sigma|M\rangle_0(\partial\langle M|\mu_\rho|G\rangle/\partial Q_t)_0 + (a^2+b^2)\langle G|\mu_\rho|M\rangle_0(\partial\langle M|\mu_\sigma|G\rangle/\partial Q_t)_0\} + \frac{1}{\upsilon_{MG}+\upsilon_t-\upsilon-i\Gamma_{Mm}}\{a^2\langle G|\mu_\sigma|M\rangle_0(\partial\langle M|\mu_\rho|G\rangle/\partial Q_t)_0 - b^2\langle G|\mu_\rho|M\rangle_0(\partial\langle M|\mu_\sigma|G\rangle/\partial Q_t)_0\}\right] \quad (4)$$

In eq 4, G and M represent ground and excited electronic states, respectively, μ_σ and μ_ρ are the dipole moment operators, υ_{MG} is the frequency difference between the indicated electronic levels, $\Gamma_{Gg'}$ and Γ_{Mm} are the damping parameters of the ground state and the Mth electronic state, respectively, and the Franck−Condon factors $a = \exp(-\Delta_t^2/2)$ and $b = -\Delta_t \exp(-\Delta_t^2/2)$ are the vibrational overlap integrals where Δ_t is a displacement of the potential energy minimum between the ground and excited states along the normal coordinate Q_t. The subscripts t in Δ_t and Q_t refer to the t vibrational mode. The electronic transition moment in eq 4 is defined as[17]

$$\mu_\rho^{GM}(\vec{r}) = \langle G|\mu_\rho|M\rangle_0 = \langle G|-e\sum_k(\vec{r}_k)_\rho|M\rangle_0 = \sqrt{2}\sum_n C_n^M\langle\varphi_{n1}(\vec{r})|-e(\vec{r})_\rho|\varphi_{n2}(\vec{r})\rangle \quad (5)$$

Here e is the charge of an electron. In the above eq 5, the ground-state electronic wave function is described by a single Slater determinant that is constructed from the SCF molecular orbitals ϕ_n and the excited-state electronic wave function is given by $|M\rangle = \sum_n C_n^M\Psi_{n1\to n2}$, where $\Psi_{n1\to n2}$ describes a singlet one-electron excitation from molecular orbitals ϕ_{n1} to ϕ_{n2}. The derivative of the electric dipole transition moment with respect to normal coordinates in eq 4 can be evaluated in the following way:[13,17]

$$\partial\mu_\rho^{GM}/\partial Q_t = (\partial\langle M|\mu_\rho|G\rangle/\partial Q_t)_0 = (\hbar/2\pi c\upsilon_t)^{1/2}\sum_{n,i,j}\sqrt{2}C_n^M\upsilon_{n1i}\upsilon_{n2j}S_{ij}\mathscr{R}_t^{j\rho}m_i^{-1/2} \quad (6)$$

where υ_{ni} is the coefficient of the atomic orbital λ_i in the molecular orbital n, the normal mode vector $\mathscr{R}_s$ defines the transformation between Cartesian coordinates and normal coordinates, and $S_{ij} = \langle\lambda_i|\lambda_j\rangle$ is the element of the overlap matrix. When the overlap integrals are taken into account, eq 6 holds even if the atom orbitals are not orthogonalized. Note that in the above Hartree−Fock scheme ϕ_n is the SCF molecule orbital. If the SCF molecule orbitals in eqs 5 and 6 are replaced by the Kohn−Sham orbitals, density functional theory can also be applied to obtain the electric dipole transition moment and its derivative.

In eq 3 the derivative of the IR transition dipole moment with respect to the normal mode Q_t is[20]

$$\frac{\partial\mu_\kappa}{\partial Q_t} = \frac{1}{\sqrt{2}}(\partial\langle G|\mu_\kappa|G\rangle/\partial Q_t)_0 \quad (7)$$

In SFVS off electronic resonance, υ_2 is near a vibrational resonance and the sum-frequency υ is far from an electronic resonance; the bulk nonlinear susceptibilities can be expressed into[13]

$$\chi_B^{chiral}(\upsilon,\upsilon_2) = \frac{N_B L_B}{6\varepsilon_0}\frac{1}{h(\upsilon_t-\upsilon_2-i\Gamma_{Gg'})}\left[\frac{\partial\mu_z}{\partial Q_t}(\alpha_{xy(3)}-\alpha_{yx(3)}) + \frac{\partial\mu_y}{\partial Q_t}(\alpha_{zx(3)}-\alpha_{xz(3)}) + \frac{\partial\mu_x}{\partial Q_t}(\alpha_{yz(3)}-\alpha_{zy(3)})\right] \quad (8)$$

where nonresonant vibrational transition polarizabilities $\alpha_{\sigma\rho(3)}$ describing vibronic coupling are[13]

$$\alpha_{\sigma\rho(3)} = \frac{1}{\sqrt{2}h}\sum_m\left\{\frac{\upsilon_t^2}{(\upsilon_{mg}-\upsilon)^3}[a^2\langle G|\mu_\rho|M\rangle_0(\partial\langle M|\mu_\sigma|G\rangle/\partial Q_t)_0 - b^2\langle G|\mu_\sigma|M\rangle(\partial\langle M|\mu_\rho|G\rangle/\partial Q_t)_0] + \frac{\upsilon_t^2}{(\upsilon_{mg}+\upsilon)^2}[3b^2\langle G|\mu_\sigma|M\rangle_0(\partial\langle G|\mu_\rho|M\rangle/\partial Q_t)_0 + (a^2+2b^2)\langle G|\mu_\rho|M\rangle_0(\partial\langle G|\mu_\sigma|M\rangle/\partial Q_t)_0]\right\} \quad (9)$$

3. Results and Discussion

It is known that in an equilibrium distribution, there are aldehydic, pyranose, and furanose isomers of arabinose introduced by mutarotation.[21] At 304 K in the D-arabinose solution the proportion of the isomers D-arabinose-aldose, α-D-arabinofuranose, α-D-arabinopyranose, β-D-arabinofuranose, and β-D-arabinopyranose are 0.03%, 2.5%, 60%, 2%, and 35.5%, respectively.[22,23] This indicates that α-D-arabinopyranose is dominant in D-arabinose solutions. And molecular structures of D-arabinose-aldose, α-D-arabinofuranose, α-D-arabinopyranose, β-D-arabinofuranose, and β-D-arabinopyranose are plotted in Figure 1.

We first discuss how to obtain the parameters used to calculate SFVS on D-arabinose solutions. Applying the density functional theory method B3LYP[24,25] and the Dunning's correlation-consistent basis set AUG-cc-pVDZ[26,27] with the Gaussian 98 program,[28] we optimize the molecular structure and calculate the fundamental IR frequencies for the five D-arabinose isomers. The computed IR frequencies are scaled by a factor of 0.9614.[29] At the same time, primitive exponents, contraction coefficients, and coordinates of each shell of atomic orbitals, molecular orbital coefficients, IR dipole moment derivatives, and Hessian matrix of force constants are obtained.

On the basis of the above optimization, TDDFT[30,31] is applied to compute excited electronic states. The calculated excitation energies and electric dipole transition moments of the five D-arabinose isomers are listed in Table 1. The energies of the first excited states for D-arabinose-aldose, α-D-arabinofuranose, α-D-arabinopyranose, β-D-arabinofuranose, and β-D-arabinopyranose are 4.4608, 6.2836, 6.1067, 6.0020, and 5.7712 eV, respectively. The first excitation energy of D-arabinose-aldose is about 1.5 eV smaller than that of the other D-arabinose isomers. The reason is that there is a C═O double bond in D-arabinose-aldose and the corresponding first excitation transition is from the n nonbond molecular orbital to the Π* antibond molecular orbital of the C═O bond and the σ* antibond molecular orbital of the C−H bond, and there is only a single bond in the other D-arabinose isomers, and their corresponding first excitation transitions are from the n nonbond orbital to the σ* antibond orbital. This is from population analysis and configuration interaction coefficients. Table 1 also shows that the oscillator strength of the first excited state for D-arabinose-aldose is very small with a value of 0.0003. The minimum of the configuration interaction coefficient computed by the Gauss-

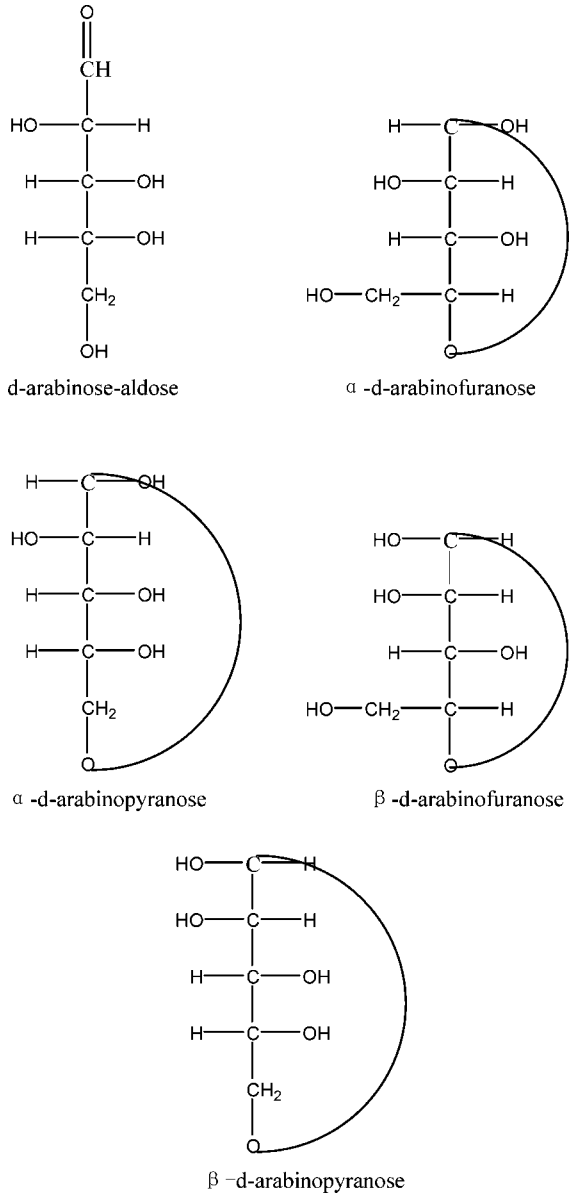

Figure 1. Molucular structures of D-arabinose-aldose, α-D-arabinofuranose, α-D-arabinopyranose, *β*-D-arabinofuranose, and *β*-D-arabinopyranose.

ian 98 program is 0.0001. Thus, configuration interaction coefficients larger than 0.0001 are taken into consideration. And in the computations for SFVS off electronic resonance the first 100 excited singlet states are taken into account.

When calculating the Franck−Condon factors, we assume that all the displacement parameters of the potential minimum of excited states are 0.1. Equations 3, 4, 8, and 9 indicate that the SFVS arise from the antisymmetric part of the Raman B term. The Raman B term is insensitive to the displacement parameter when $\Delta_t \ll 1$.[12,13] All the IR line widths are taken as 12 cm^{-1}, and all the Lorentz local field correction factors are taken to be unity.

3.1. Theoretical Doubly Resonant IR−UV SFVS of D-Arabinose Solutions. On the basis of the TDDFT//B3LYP/AUG-cc-pVDZ results and using eqs 3−7, we calculate the doubly resonant IR−UV SFVS $|\chi_B^{chiral}/N_B|^2$ for vibrational modes of the five D-arabinose isomers with sum-frequency (SF) resonant to the first singlet excited state and the second singlet excited state, respectively. The calculated results are plotted in Figure 2. Because the concentration of α-D-arabinopyranose is

TABLE 1: Calculated Excited-State Energies (eV), Electric Dipole Transition Moments (au), and Oscillator Strengths for the Excited Singlet States of D-Arabinose-aldose, α-D-Arabinofuranose, α-D-Arabinopyranose, *β*-D-Arabinofuranose, and *β*-D-Arabinopyranose Molecules Using the TDDFT//B3LYP/AUG-cc-pVDZ Method

state	excitation energies	$\langle i\|x\|0\rangle$	$\langle i\|y\|0\rangle$	$\langle i\|z\|0\rangle$	*f*
		D-Arabinose-aldose			
1 (A)	4.4608	0.0442	0.0220	0.0238	0.0003
2 (A)	5.4107	−0.4195	−0.0672	0.0464	0.0242
3 (A)	5.8487	0.2216	−0.0208	−0.0010	0.0071
4 (A)	6.1040	−0.1404	−0.0127	0.0223	0.0030
5 (A)	6.2008	−0.1384	−0.0278	−0.0867	0.0042
6 (A)	6.3632	0.0125	0.0731	−0.2345	0.0094
		α-D-Arabinofuranose			
1 (A)	6.2836	0.0385	0.0147	0.1009	0.0018
2 (A)	6.3138	−0.0678	−0.1107	−0.1178	0.0048
3 (A)	6.496	−0.0497	0.1184	0.0157	0.0027
4 (A)	6.6151	0.2935	−0.2249	0.0595	0.0227
5 (A)	6.6525	−0.2081	0.0566	0.0322	0.0078
6 (A)	6.7541	−0.0479	0.0800	−0.0711	0.0023
		α-D-Arabinopyranose			
1 (A)	6.1067	0.1195	0.0119	0.2128	0.0089
2 (A)	6.3725	0.0676	0.0305	0.2463	0.0103
3 (A)	6.5272	−0.0578	−0.1061	−0.0846	0.0035
4 (A)	6.5494	0.1338	−0.0671	0.2072	0.0105
5 (A)	6.7198	−0.0865	0.0846	−0.2272	0.0109
6 (A)	6.8324	0.1989	0.0040	−0.1160	0.0089
		β-D-Arabinofuranose			
1 (A)	6.0020	−0.2266	−0.1569	0.1449	0.0143
2 (A)	6.2353	−0.0646	0.0767	0.0131	0.0016
3 (A)	6.3930	−0.0494	−0.0022	0.1196	0.0026
4 (A)	6.4837	−0.0032	−0.2310	−0.0208	0.0085
5 (A)	6.5720	0.0392	0.2523	−0.2082	0.0175
6 (A)	6.6123	0.1771	−0.0677	−0.1687	0.0104
		β-D-Arabinopyranose			
1 (A)	5.7712	−0.0224	0.1617	0.0786	0.0046
2 (A)	6.0158	0.1164	−0.0193	0.0795	0.0030
3 (A)	6.4283	−0.0454	0.0210	0.0690	0.0011
4 (A)	6.512	0.0560	−0.1418	0.2600	0.0145
5 (A)	6.5703	−0.0169	0.0200	−0.0368	0.0003
6 (A)	6.6422	0.0750	0.1374	0.1203	0.0063

maximal in D-arabinose solutions, we consider its SFVS first. When the sum-frequency is resonant with the first excited state with an oscillator strength of 0.0089, the most intense peak strength $|\chi_B^{chiral}/N_B|^2$ of the chiral spectra for α-D-arabinopyranose is 2.0×10^{-77} m^8/V^2 at 1063 cm^{-1}. The concentration of the water solution of D-arabinose is 2.46 M,[3] i.e., $N_B = 1.48 \times 10^{27}$ m^{-3}. Thus, the most intense peak strength $|\chi_B^{chiral}|^2$ is 1.6×10^{-23} m^2/V^2. Ref 8 shows that the SFVS with peak strength of 10^{-29} m^2/V^2 can be detectable. The peak strength of chiral spectra for α-D-arabinopyranose is about 6 orders of magnitude stronger than the detection limit; hence, chiral spectra of α-D-arabinopyranose resonant with the first excited state can be easily detected. Also, chiral spectra of α-D-arabinopyranose resonant with the second excited state is in the order of magnitude of 10^{-24} m^2/V^2 and can also be measurable. Similarly, the most intense peak strengths of the chiral spectra for D-arabinose-aldose, α-D-arabinofuranose, *β*-D-arabinofuranose, and *β*-D-arabinopyranose resonant with the first excited state are 1.7×10^{-80} (3.3×10^{-33}), 2.5×10^{-78} (3.4×10^{-27}), 4.7×10^{-78} (4.1×10^{-27}), and 4.9×10^{-78} m^8/V^2 (1.4×10^{-24} m^2/V^2), respectively, and all of their chiral spectra can be detected except D-arabinose-aldose. The reason is that both the oscillator strength (0.0003) of the first excited state and the concentration (0.000738 M) for D-arabinose-aldose are very small. When the sum-

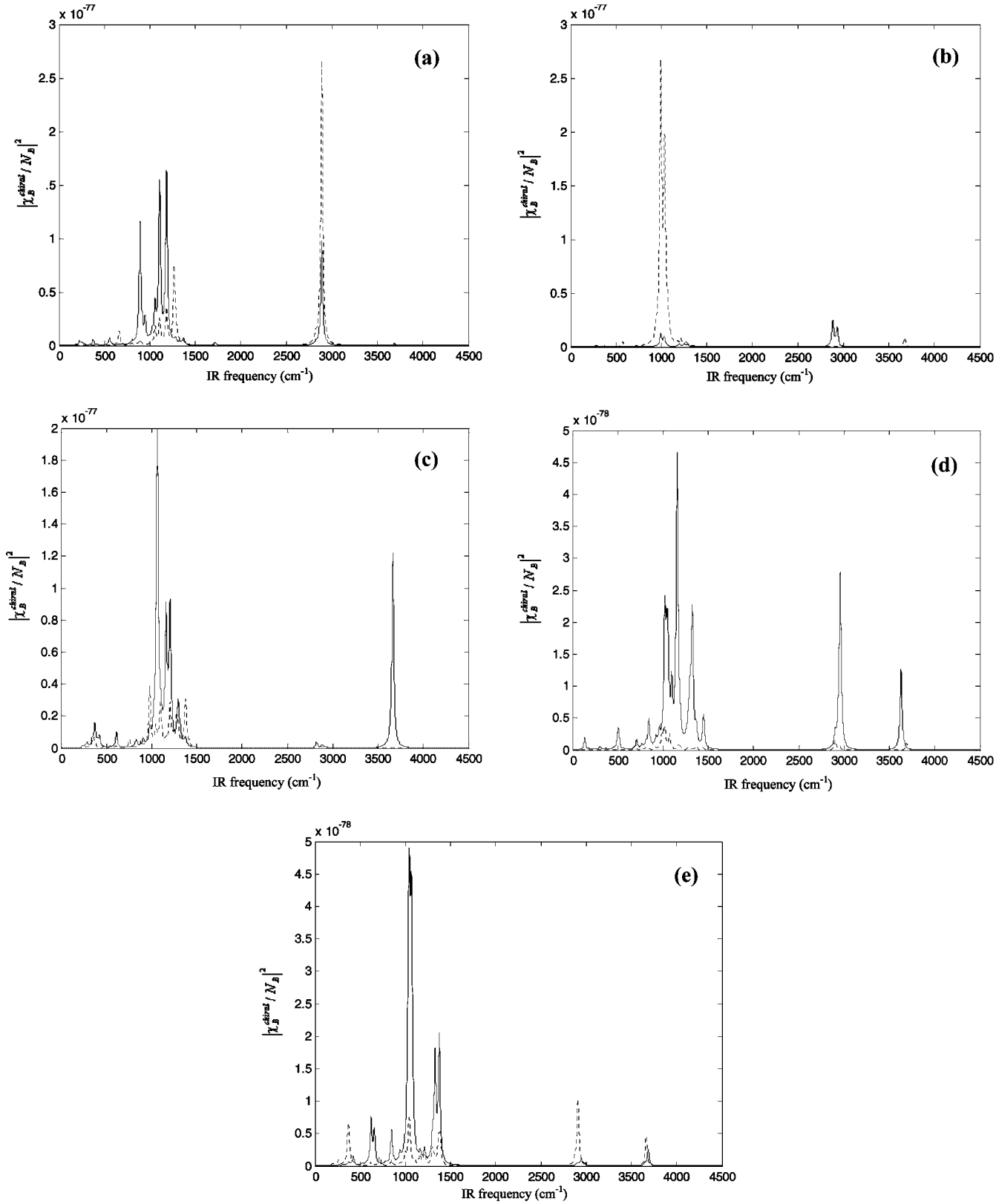

Figure 2. Calculated chiral spectra $|\chi_B^{chiral}/N_B|^2$ (m^8/V^2) resonant to the first excited state (solid line) and the second excited state (dotted line) for vibrational modes of (a) D-arabinose-aldose with sum-frequency (SF) at 4.4608 and 5.4107 eV (the dotted line is multiplied by a factor of 1000), (b) α-D-arabinofuranose with SF at 6.2836 and 6.3138 eV, (c) α-D-arabinopyranose with SF at 6.1067 and 6.3725 eV, (d) β-D-arabinofuranose with SF at 6.0020 and 6.2353 eV, and (e) β-D-arabinopyranose with SF at 5.7712 and 6.0158 eV, respectively.

frequency is resonant with the second excited state, the most intense peak strengths of the chiral spectra for D-arabinose-aldose, α-D-arabinofuranose, α-D-arabinopyranose, β-D-arabinofuranose, and β-D-arabinopyranose are 2.7×10^{-77} (5.3×10^{-30}), 2.7×10^{-77} (3.6×10^{-26}), 3.9×10^{-78} (3.1×10^{-24}), 3.8×10^{-79} (3.3×10^{-28}), and 1.1×10^{-78} m^8/V^2 (3.0×10^{-25} m^2/V^2). Thus, the chiral spectra for α-D-arabinofuranose, α-D-arabinopyranose, β-D-arabinofuranose, and β-D-arabinopyranose

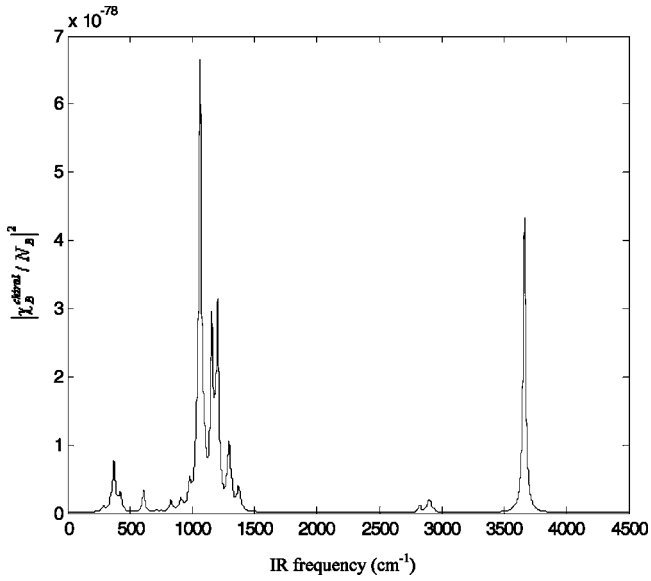

Figure 3. Calculated chiral spectra $|\chi_B^{chiral}/N_B|^2$ (m^8/V^2) of D-arabinose solutions resonant to the first two excited states with SF at 6.1 eV.

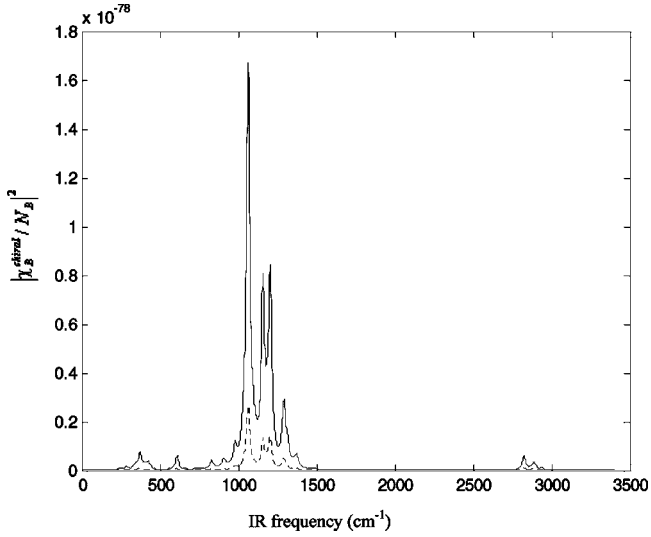

Figure 4. Calculated chiral spectra $|\chi_B^{chiral}/N_B|^2$ (m^8/V^2) resonant to the first excited state for α-D-arabinopyranose with SF at 6.0 eV (solid line) and 5.9 eV (dotted line), respectively.

can be measurable and it is hard to detect chiral spectra for D-arabinose-aldose. In Figure 3, we plot chiral spectra of D-arabinose solutions resonant to the first two excited states with SF at 6.1 eV. This SF approaches the energy (6.1067 eV) of the first excited state of α-D-arabinopyranose, and the line shape of the complete spectra is similar to that of α-D-arabinopyranose. The spectra weighted by the knowledge of isomer distributions can be in the order of magnitude of 10^{-77} m^8/V^2 and are intense enough to be detected.

We also study the absorption of the doubly resonant SFVS. In Figure 4, the chiral spectra resonant to the first excited state for α-D-arabinopyranose with SF at 6.0 and 5.9 eV are plotted, respectively. The spectra of 6.0 eV are of the order of magnitude of 10^{-78} m^8/V^2 and 1 order of magnitude smaller than those of 6.1067 eV, and the spectra of 5.9 eV are 2 orders of magnitude smaller than those of 6.1067 eV. When the sum-frequency is away from the resonance frequency, the spectra intensity decreases much. Also, in Figure 5 we show the peak strengths of the chiral spectra for the 1063 cm^{-1} vibrational mode of α-D-arabinopyranose versus the SF around the resonance to the first

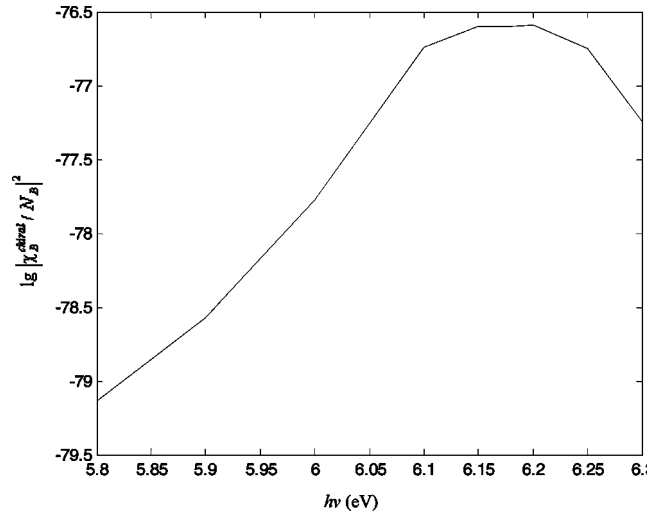

Figure 5. Calculated peak strengths of the chiral spectra $|\chi_B^{chiral}/N_B|^2$ (m^8/V^2) for the vibrational mode of α-D-arabinopyranose at 1063 cm^{-1} vs the SF around the resonance to the first excited state.

TABLE 2: Calculated IR Frequencies (cm^{-1}) (Scaled by a Factor of 0.9614), IR Intensities (km/mol), Doubly Resonant Sum-Frequency Vibrational Spectroscopy (SFVS) (10^{-78} m^8/V^2), Relative Values of Isotropic, Antisymmetric, and Anisotropy Tensor Invariants Due to the Raman B Term for the Vibrational Modes of α-D-Arabinopyranose with TDDFT//B3LYP/AUG-cc-pVDZ Computations and the Input UV Frequency Fixed at 6.1067 eV

IR frequency	1058	1063	1096	1157	1184	1204	1292
IR intensity	52.4	210	72.9	45.9	50.4	52.0	9.17
SFVS	2.56	17.1	1.31	7.96	1.31	8.24	1.79
Σ^0	0.407	0.031	0.001	0.011	0.423	0.164	0.048
Σ^1	0.124	0.212	0.097	0.391	0.081	0.454	0.555
Σ^2	1.06	0.477	0.187	0.732	0.990	1.12	1.02

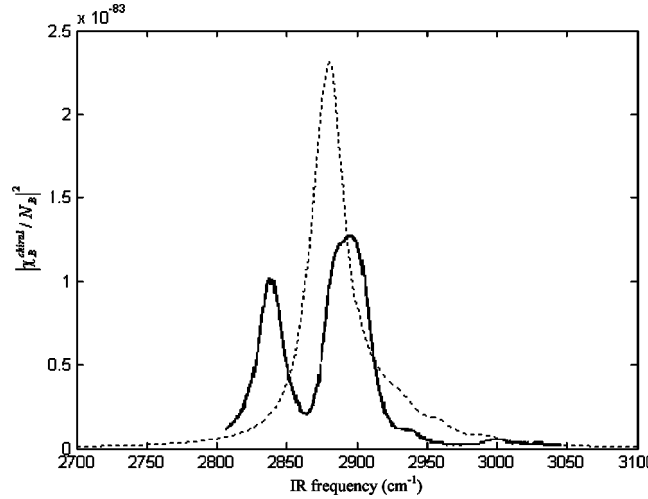

Figure 6. Calculated sum-frequency vibrational spectroscopy $|\chi_B^{chiral}/N_B|$ (m^8/V^2) (dotted line) of (*R*)-limonene in the range of 2700−3200 cm^{-1} with the input visible beam fixed at 532 nm; the experimental spectroscopy curve (solid line) from Figure 3 of ref 8 is also shown.

excited state. It is interesting that the most intense peak strength is not at 6.1067 eV of the first excited state but at 6.2 eV, which may due to Franck−Condon progression.

In order to obtain the antisymmetric vibrational transition polarizabilities that contribute to the SFVS, we calculate SFVS, IR intensities, isotropic, antisymmetric, and anisotropy tensor invariants due to the Raman B term for the vibrational modes

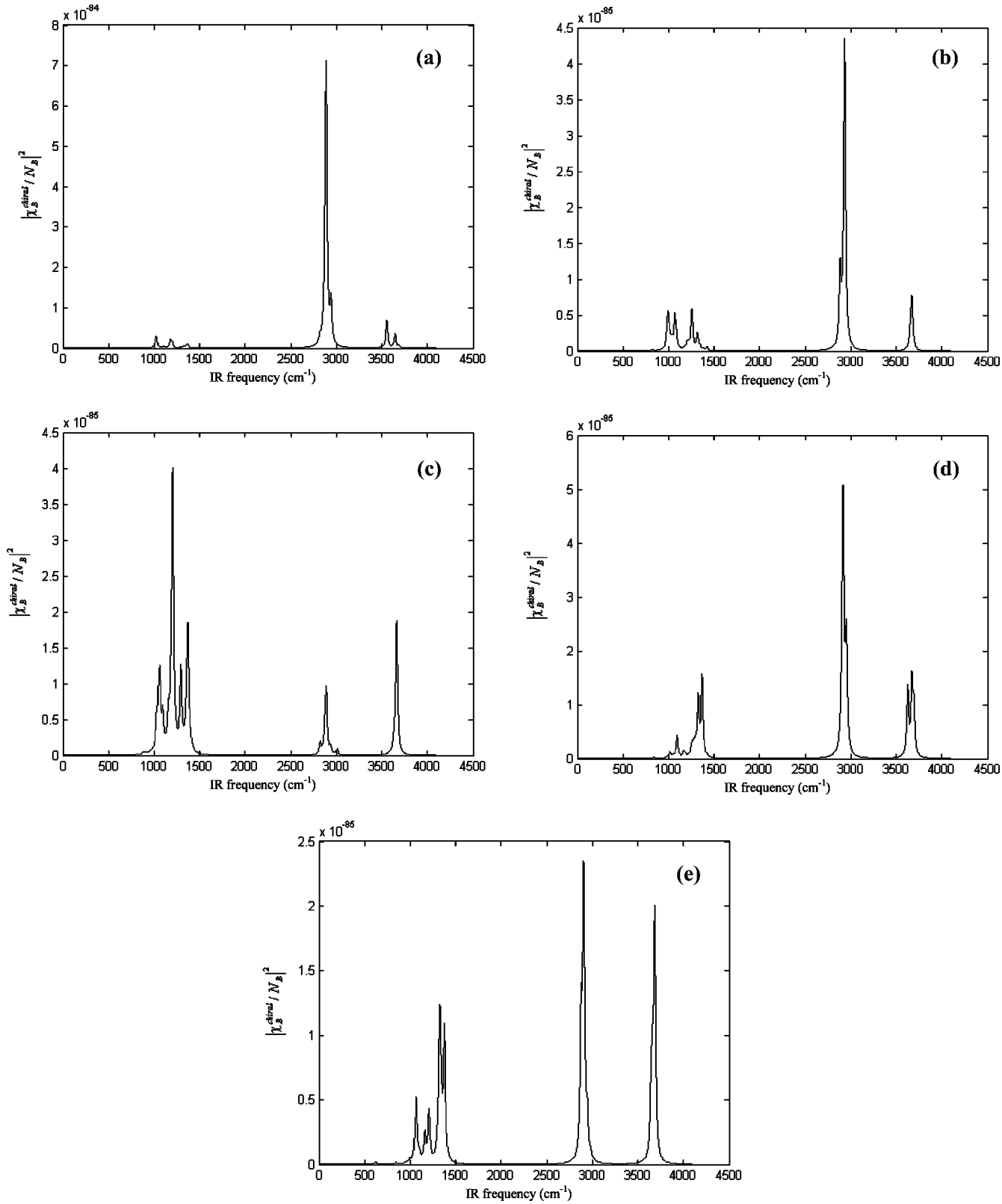

Figure 7. Calculated sum-frequency vibrational spectroscopy $|\chi_B^{chiral}/N_B|$ (m^8/V^2) of (a) D-arabinose-aldose, (b) α-D-arabinofuranose, (c) α-D-arabinopyranose, (d) β-D-arabinofuranose, and (e) β-D-arabinopyranose with the input visible beam fixed at 532 nm.

of α-D-arabinopyranose with the input UV beam fixed at 6.1067 eV resonant to the first excited state (see Table 2). The SFVS of the 1063 cm^{-1} mode is most intense, and the IR intensity is largest with a value of 210 km/mol, and its corresponding isotropic, antisymmetric, and anisotropy tensor invariants are 0.031, 0.212, and 0.477, respectively, which shows that antisymmetric and anisotropy tensor invariants can be of the same order of magnitude only from the contribution of the Raman B term. However, antisymmetric tensor invariants of the 1063 cm^{-1} mode are smaller than those of the 1157, 1204, and 1292 cm^{-1} vibrational modes. In a resonant case, the Raman A term contributes to symmetric tensor invariants but not to antisymmetric tensor invariants for nondegenerate vibrational modes. Thus, antisymmetric tensor invariants do not change and

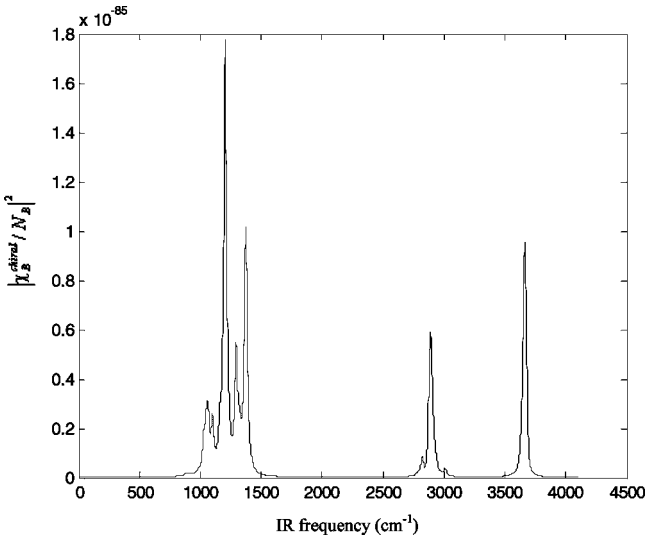

Figure 8. Calculated sum-frequency vibrational spectroscopy $|\chi_B^{chiral}/N_B|$ (m^8/V^2) of D-arabinose solutions with the input visible beam fixed at 532 nm.

TABLE 3: Calculated IR Frequencies (cm^{-1}) (Scaled by a Factor of 0.9614), IR Intensities (km/mol), Sum-Frequency Vibrational Spectroscopy (SFVS) Off Electronic Resonance (10^{-85} m^8/V^2), Relative Values of Isotropic, Antisymmetric, and Anisotropy Tensor Invariants, and the Depolarization Ratio for the Vibrational Modes of α-D-Arabinopyranose with TDDFT//B3LYP/AUG-cc-pVDZ Computations and the Input Visible Beam Fixed at 532 nm

IR frequency	1204	1366	2889	3663
IR intensity	52.0	18.9	110	78.9
SFVS	3.80	1.19	0.864	1.09
Σ^0	0.00003	0.00008	0.0126	0.00119
Σ^1	1.57×10^{-9}	1.12×10^{-9}	1.02×10^{-9}	4.16×10^{-9}
Σ^2	0.01404	0.00158	0.01295	0.00185
ρ	0.746	0.666	0.219	0.287

isotropic and anisotropy tensor invariants change when the Raman A term is considered.

Theoretical studies indicate that doubly resonant IR−UV SFVS spectra of D-arabinose solutions can be detectable only if the sum-frequency is resonant to the excited states of α-D-arabinofuranose, α-D-arabinopyranose, β-D-arabinofuranose, or β-D-arabinopyranose with large electric dipole transition moments. However, The deep UV above 5.6 eV light generated by the high-energy electronic states would be strongly absorbed by most window materials and by air itself. It is difficult that such experiments will be performed in the near future because of these formidable practical challenges.

3.2. Computations on SFVS Off Electronic Resonance for D-Arabinose Solutions. In order to prove that TDDFT//B3LYP/AUG-cc-pVDZ computations can be applied to estimate the magnitude of the intensity for SFVS off electronic resonance, using eqs 8, 9, and 5−7 the SFVS off electronic resonance for (*R*)-limonene liquids in the range of 2700−3100 cm^{-1} with the input visible beam fixed at 532 nm are computed. The calculated results are plotted in Figure 6. Experiment[8] shows that the SFVS for the 2839 and 2905 cm^{-1} vibrational modes are 1.0×10^{-83} and 1.2×10^{-83} m^8/V^2, respectively. The SFVS for these two modes are most intense. The corresponding calculated vibrational frequencies are 2873 and 2882 cm^{-1} with the SFVS of 8.1×10^{-84} and 1.6×10^{-83} m^8/V^2, respectively. The two calculated vibrational frequencies are close, and the calculated SFVS show only one strong peak in Figure 3. However, both the calculated vibrational frequencies and the intensities of the calculated SFVS agree with experiment qualitatively.[8] Thus, TDDFT//B3LYP/AUG-cc-pVDZ can be applied to estimate the magnitude of SFVS off electronic resonance.

Using TDDFT//B3LYP/AUG-cc-pVDZ, we calculate the SFVS off electronic resonance $|\chi_B^{chiral}/N_B|^2$ for the five D-arabinose isomers with the frequency of the input visible beam fixed at 532 nm. The calculated results are plotted in Figures 7 and 8. Figure 7 shows the SFVS of the individual isomer, and Figure 8 shows the complete SFVS for D-arabinose solutions appear in the range of 0−4500 cm^{-1}. The most intense peak strengths of the SFVS off electronic resonance for D-arabinose-aldose, α-D-arabinofuranose, α-D-arabinopyranose, β-D-arabinofuranose, and β-D-arabinopyranose are 7.1×10^{-84} (1.4×10^{-36}), 4.4×10^{-85} (6.0×10^{-34}), 4.0×10^{-85} (3.2×10^{-31}), 5.1×10^{-85} (4.5×10^{-35}), and 2.3×10^{-85} m^8/V^2 (6.3×10^{-32} m^2/V^2), respectively. The intensity of SFVS for D-arabinose solutions can be the order of magnitude of 10^{-31} m^2/V^2, which is 2 orders of magnitude smaller than SFVS detection limit. Thus, it may be difficult to observe the SFVS off electronic resonance from D-arabinose solutions.

In Table 3, we list SFVS, IR intensities, isotropic, antisymmetric, anisotropy tensor invariants, and the depolarization ratio for the vibrational modes of α-D-arabinopyranose with the frequency of the input visible beam fixed at 532 nm. In a nonresonant case, the Raman A term is zero even for totally symmetric vibrational modes and only the Raman B term contributes to Raman scattering. The SFVS of the 1204 cm^{-1} vibrational mode is most intense with an IR intensity of 52.0 km/mol. This IR intensity is not the largest one and is smaller than 110 km/mol of the 2889 cm^{-1} mode. The isotropic, antisymmetric, and anisotropy tensor invariants of the 1204 cm^{-1} mode are 0.00003, 1.57×10^{-9}, and 0.01404, respectively. Antisymmetric tensor invariants are 7 orders of magnitude smaller than anisotropy ones. The depolarization ratio of this mode is 0.746, which is very close to 0.75. This is due to the small isotropic and antisymmetric tensor invariants.

From the above discussion, resonance in the sum-frequency has a large effect on the magnitude of antisymmetric vibrational Raman polarizabilities. First, the origins of the antisymmetric resonant and nonresonant vibrational Raman polarizabilities are somewhat different; though for chiral molecules the Raman B term contributes to both antisymmetric polarizabilities, antisymmetric nonresonant Raman polarizabilities from the Raman B term are almost zero with an error 10^{-4} times as large as symmetric transition polarizabilities[32] when all the vibrational states of the excited state are taken into consideration; hence, antisymmetric nonresonant Raman polarizabilities from the Raman D term beyond the Born−Oppenheimer approximation can be of the same order of magnitude of those from the Raman B term;[33] however, antisymmetric resonant Raman polarizabilities can be of the same order of magnitude of symmetric ones. Second, in resonant cases polarizabilities are approximatively inversely proportional to line width with a value of 500 cm^{-1}, and in nonresonant cases polarizabilities are inversely proportional to the frequency difference between the sum-frequency and the excited energies with a value of more than 25 000 cm^{-1}. Thus, antisymmetric resonant vibrational Raman polarizabilities are much larger than nonresonant ones.

In Tables 2 and 3, the Placzek invariants Σ^0, Σ^1, and Σ^2 are defined as[34]

$$\Sigma^0 = \frac{1}{3}|\alpha_{xx} + \alpha_{yy} + \alpha_{zz}|^2$$

$$\Sigma^1 = \frac{1}{2}\{|\alpha_{xy} - \alpha_{yx}|^2 + |\alpha_{xz} - \alpha_{zx}|^2 + |\alpha_{yz} - \alpha_{zy}|^2\}$$

$$\Sigma^2 = \frac{1}{2}\{|\alpha_{xy} + \alpha_{yx}|^2 + |\alpha_{xz} + \alpha_{zx}|^2 + |\alpha_{yz} + \alpha_{zy}|^2\} + \frac{1}{3}\{|\alpha_{xx} - \alpha_{yy}|^2 + |\alpha_{xx} - \alpha_{zz}|^2 + |\alpha_{yy} - \alpha_{zz}|^2\} \quad (10)$$

Thus, Σ^0 is the isotropic part of the Raman tensor and Σ^2 is the symmetric anisotropy, whereas Σ^1 refers to the antisymmetric part of the tensor. Also, the depolarization ρ describing the polarization properties can be expressed into[34]

$$\rho = \frac{5\Sigma^1 + 3\Sigma^2}{10\Sigma^0 + 4\Sigma^2} \quad (11)$$

4. Conclusions

The doubly resonant IR−UV sum-frequency vibrational spectroscopy and sum-frequency vibrational spectroscopy off electronic resonance for the five D-arabinose isomers in solutions are investigated using the time-dependent density functional theory. When the sum-frequency is resonant with the first and second excited states of α-D-arabinofuranose, α-D-arabinopyranose, β-D-arabinofuranose, or β-D-arabinopyranose, the calculated doubly resonant IR−UV SFVS spectra are larger than the experimental detection limit and can be detected. However, the SFVS off electronic resonance for D-arabinose solutions with the input visible beam fixed at 532 nm is 2 orders of magnitude smaller than the SFVS detection limit, which may be undetectable.

Acknowledgment. This work is supported by the Natural Science Foundation for University of Anhui Province (No. KJ2008B170).

References and Notes

(1) Buckingham, A. D. In *Optical, Electric and Magnetic Properties of Molecules—A Review of the Work of A. D. Buckingham*; Clary, D. C., Orr, B. J., Eds.; Elsevier: Amsterdam, The Netherlands, 1997.
(2) Barron, L. D. *Molecular Light Scattering and Optical Activity*, 2nd ed.; Cambridge University Press: Cambridge, U.K., 2004.
(3) Fischer, P.; Wiersma, D. S.; Righini, R.; Champagne, B.; Buckingham, A. D. *Phys. Rev. Lett.* **2000**, *85*, 4253.
(4) Fischer, P.; Buckingham, A. D.; Beckwitt, K.; Wiersma, D. S.; Wise, F. W. *Phys. Rev. Lett.* **2003**, *91*, 173901.
(5) Fisher, P.; Hache, F. *Chirality* **2005**, *17*, 421.
(6) Fischer, P.; Wise, F. W.; Albrecht, A. C. *J. Phys. Chem. A* **2003**, *107*, 8232.
(7) Belkin, M. A.; Shen, Y. R. *Int. Rev. Phys. Chem.* **2005**, *24*, 257.
(8) Belkin, M. A.; Kulakov, T. A.; Ernst, K. H.; Yan, L.; Shen, Y. R. *Phys. Rev. Lett.* **2000**, *85*, 4474.
(9) Belkin, M. A.; Han, S.-H.; Wei, X.; Shen, Y. R. *Phys. Rev. Lett.* **2001**, *87*, 113001.
(10) Belkin, M. A.; Shen, Y. R. *Phys. Rev. Lett.* **2003**, *91*, 213907.
(11) Moad, A. J.; Simpson, G. J. *J. Phys. Chem. B* **2004**, *108*, 3548.
(12) Zheng, R.-H.; Chen, D.-M.; Wei, W.-M.; He, T.-J.; Liu, F.-C. *J. Phys. Chem. B* **2006**, *110*, 4480.
(13) Zheng, R.-H.; Wei, W.-M. *J. Phys. Chem. B* **2007**, *116*, 1431.
(14) Giordmaine, J. A. *Phys. Rev.* **1965**, *138*, A1599.
(15) Rentzepis, P. M.; Giordmaine, J. A.; Wecht, K. W. *Phys. Rev. Lett.* **1966**, *16*, 792.
(16) Shkurinov, A. P.; Dubrovskii, A. V.; Koroteev, N. I. *Phys. Rev. Lett.* **1993**, *70*, 1085.
(17) Warshel, A.; Dauber, P. *J. Chem. Phys.* **1977**, *66*, 5477.
(18) Warshel, A. *Annu. Rev. Biophys. Bioeng.* **1977**, *6*, 273.
(19) Fischer, P.; Buckingham, A. D.; Albrecht, A. C. *Phys. Rev. A* **2001**, *64*, 053816.
(20) Komornicki, A.; Jaffe, R. L. *J. Chem. Phys.* **1979**, *71*, 2150.
(21) Tipson, R. S.; Isbell, H. S. *J. Res. Natl. Bur. Stand.* **1962**, *66A*, 31.
(22) Angyal, S. J. *Adv. Carbohydr. Chem. Biochem.* **1984**, *42*, 15.
(23) Angyal, S. J. *Adv. Carbohydr. Chem. Biochem.* **1991**, *49*, 19.
(24) Lee, C.; Yang, W.; Parr, R. G. *Phys. Rev. B* **1988**, *37*, 785.
(25) Becke, A. D. *J. Chem. Phys.* **1993**, *98*, 5648.
(26) Woon, D. E.; Dunning, T. H., Jr. *J. Chem. Phys.* **1993**, *98*, 1358.
(27) Kendall, R. A.; Dunning, T. H., Jr.; Harrison, R. J. *J. Chem. Phys.* **1992**, *96*, 6796.
(28) Frisch, M. J.; et al. Gaussian 98, revision A.11; Gaussian Inc.: Pittsburgh, PA, 1998.
(29) Halls, M. D.; Velkovski, J.; Schlegel, H. B. *Theor. Chem. Acc.* **2001**, *105*, 413.
(30) Bauernschmitt, R.; Ahlrichs, R. *Chem. Phys. Lett.* **1996**, *256*, 454.
(31) Casida, M. E.; Jamorski, C.; Casida, K. C.; Salahub, D. R. *J. Chem. Phys.* **1998**, *108*, 4439.
(32) Liu, F.-C. *J. Phys. Chem.* **1991**, *95*, 7180.
(33) Belkin, M. A.; Shen, Y. R.; Harris, R. A. *J. Chem. Phys.* **2004**, *120*, 10118.
(34) Mortensen, O. S.; Hassing, S. *Adv. Infrared Raman Spectrosc.* **1980**, *6*, 1.

JP808228E